NEW CARBON MATERIALS
Volume 26, Issue 3, Jun 2011
Online English edition of the Chinese language journal

Available online at www.sciencedirect.com
ScienceDirect

Cite this article as: New Carbon Materials, 2011, 26(3):197–203.

RESEARCH PAPER

A comparative study of nitrogen-doped hierarchical porous carbon monoliths as electrodes for supercapacitors

HAO Guang-ping, MI Juan, LI Duo, QU Wen-hui, WU Ting-jun, LI Wen-cui*, LU An-hui*

State Key Laboratory of Fine Chemicals, School of Chemical Engineering, Dalian University of Technology, Dalian 116024, China

Abstract: Two nitrogen-doped carbon monoliths with hierarchical porosity over a large size range were prepared by polymerization of resorcinol and formaldehyde in the presence of an organic amine, L-lysine, and an inorganic base, ammonium hydroxide under ambient conditions. Their physical and chemical features were characterized by N_2 sorption, transmission and scanning electron microscopy, and elemental analysis. Their electrochemical properties as the electrodes of supercapacitors were evaluated under both a three-electrode system and a two-electrode system. Results show that the two types of nitrogen-doped carbon possess similar pore structures, but have distinct electrochemical performances. The L-lysine incorporated carbon monolith has a high nitrogen content, a high specific capacitance of 199 $F \cdot g^{-1}$, and a 1.6% loss in the specific capacitance after 1000 charge-discharge cycles, indicating a long-term cycling stability.

Key Words: Carbon; Hierarchical porosity; Nitrogen-doped; Supercapacitor; Electrochemical properties

1 Introduction

Electric double-layer capacitors (EDLCs), also called supercapacitors or ultracapacitors, have attracted great interest in energy storage, owing to their large power capability, high efficiency, and long cycle life[1]. EDLCs store charge in the double layer formed at the electrolyte-electrode interface when voltage is applied. The electrodes are generally composed of high-surface-area conductive material, usually porous carbons and carbon-based hybrid composites[2] having high specific surface area, controllable pore structure, and tunable surface chemistry[3-4]. In recent years, various types of carbons, including activated carbons[5-6], carbon aerogels[7-8], templated carbons[9-13], and carbon fibers/nanotubes[14-16] have been prepared and investigated as sole electrode component or as part of composite electrodes that contain pseudocapacitance materials for EDLCs. The capacitance of EDLC can be expressed as the equation [17]:

$$C = \frac{\varepsilon_r \times \varepsilon_0 \times A}{d},$$

where ε_r and ε_0 are the electrolyte dielectric constants, A is the electrode surface area, and d is the distance between electrolyte ions and carbon. According to this equation, the carbons with high surface areas and proper pore structures are suitable for the EDLC electrodes. Besides, physical characteristics such as good intra- and interparticle conductivity in porous matrices, high electrolyte accessibility to intrapore surface, and good bulk electrical conductivity are also highly desirable. It is commonly believed that coexistence of larger mesopores and/or macropores with micropores in carbons is required for rapid ion transport or high power density of EDLCs[18-19]. In addition, decorating nitrogen atoms in the carbon matrix have been proved to be an effective way to improve its wettability, and to contribute an additional capacitance[20-22]. Yang and coworkers find that a 3-D continuous pore structure and a high nitrogen content are beneficial to fast ion transport, high pseudocapacitance, and good wettability[23].

Thus, researchers usually assume that carbon materials with N-doped frameworks and hierarchical porosity are required for a superior electrode material for EDLC applications. Using heteroatom-containing precursors in the synthesis of porous carbon is a useful way to incorporate heteroatoms into carbon[24]. The variety of possible organic precursors containing heteroatoms is very large, and their final products are also various because of different char yield and heteroatom content. This inspired many researchers to create different nitrogen-doped carbons by designing nitrogen-containing precursors, and then to investigate their electrochemical properties. Until now, several works have been reported on electrochemical properties of N-doped porous carbons (mainly powder or film) prepared mainly through nanocasting techniques[13,23]. To our knowledge, there are still few works about a direct synthesis of nitrogen-doped carbon monoliths and the evaluation of their electrochemical properties.

Herein, we report a comparative study of electrochemical performances of two types of nitrogen-doped hierarchical

Received date: 3 May 2011; **Revised date:** 6 June 2011
***Corresponding author.** E-mail: wencuili@dlut.edu.cn; anhuilu@dlut.edu.cn

DOI: 10.1016/S1872-5805(11)60076-0

porous carbons, which are obtained by a one-step process using different nitrogen-containing molecules, an organic amine, L-lysine, and an inorganic base, ammonium, as catalysts. Both of the two nitrogen-doped carbon monoliths obtained possess a hierarchical porosity with similar three-dimensional (3-D) bicontinuous morphologies, surface areas, and micropore fractions; however, they demonstrate a distinct electrochemical behavior.

2 Experimental

2.1 Synthesis of nitrogen-doped hierarchical porous carbon monoliths

As described in a previous publication[25], the nitrogen-doped hierarchical porous carbon monoliths were synthesized by copolymerization of resorcinol and formaldehyde in the presence of L-lysine or ammonium at ambient conditions. In a typical procedure, 1.5 g of resorcinol was dissolved in 5 mL water to form a clear solution to which 2.21 g of formaldehyde (37% by mass fraction) was added during stirring, resulting in solution A. Solution B contained 0.5 g of L-lysine dissolved in 2.5 mL of water. Solution A was quickly decanted into solution B, and within 1 min, a yellow bulk polymer was formed and further cured at 90 ºC for an additional 4 h. Finally, a porous carbon monolith (denoted C-1) was obtained by pyrolysis of the polymer at 800 ºC for 2 h, with a heating rate of 5 ºC·min^{-1}. In another run, the inorganic base, ammonium was used instead of L-lysine to synthesize another porous carbon sample while the other parameters and procedures were maintained the same. The final porous carbon obtained was denoted as C-2. It should be noted that the ammonium-catalyzed polymerization lasted for a much longer time than that of C-1.

2.2 Characterizations

Transmission electron microscopic (TEM) images of the samples were obtained with a Tecnai G^{2}20S-Twin electron microscope equipped with a cold field emission gun. The acceleration voltage was 200 kV. Samples were prepared by dropping a few drops of a suspension of one sample in ethanol onto the holey carbon grid with a pipette. Scanning electron microscopic (SEM) investigations were carried out with a Hitachi S-4800 instrument. Nitrogen sorption isotherms were measured with a TriStar 3000 adsorption analyzer (Micromeritics) at liquid nitrogen temperature. The Brunauer-Emmett-Teller (BET) method was utilized to calculate the specific surface areas (S_{BET}). The total pore volumes were estimated from the adsorbed amount at a relative pressure p/p_0 of 0.997. Micropore volume (v_{micro}) was calculated using the t-plot method. The mesopore volume (v_{meso}) was obtained by deduction of micropore volume from the total pore volume. Nitrogen content analysis was carried out on a CHNO elemental analyzer (Vario EL III, Elementar). The sample was first digested at a high temperature with subsequent scrubbing of nonanalytes from the combustion gases. The analyte gases were transported in helium carrier stream. After reduction of the formed nitrogen oxides, the gas mixture was separated into its components, which were sequentially released to a thermal conductive detector (TCD). Furthermore, the percent content of nitrogen was calculated from the detector signal in connection with the sample weight and the stored calibration curve.

2.3 Electrochemical measurements

The working electrodes were prepared by mixing mass fraction 90% active material and 10% polytetrafluoroethylene (PTFE) in 7 mL ethanol followed by an ultrasonication treatment for 20 min. The slurry of the mixture was put onto a nickel foam current collector with an area of 1 cm^2 and pressed under a pressure of 10 MPa for 5 min to fabricate an electrode. The mass loading of the active materials was ca. 5 mg·cm^{-2}. Cyclic voltammmetry (CV) and galvanostatic charge/discharge cycling (GC) were employed in the evaluation of capacitance of each sample. The performance of a single electrode was tested on CHI602C/606C electrochemical workstation. Both CV and GC experiments were carried out at room temperature under flowing nitrogen with a conventional three-electrode electrochemical setup, in which the active materials electrode served as working electrode, and a platinum plate and Hg/HgO were used as counter electrode and reference electrode, respectively. 6 mol·L^{-1} KOH was used as the electrolyte. Besides evaluation in the three-electrode system, a supercapacitor was constructed by two symmetric working electrodes using a membrane filter (MPF50AC) as a separator, and measured using an Arbin SCTS-165699-T multi-channel electrochemical workstation. The specific gravimetric capacitance based on single electrode was calculated from the galvanostatic discharge curve of the fifth cycle[1], according to equation 1:

$$C = \frac{I\Delta t}{m\Delta V}, \tag{1}$$

Where C(F·g^{-1}), I (A), ΔV (V), Δt (s), and m (g) are the specific gravimetric capacitance, the discharge current, the potential window during the discharge process, the discharge time interval within the potential window, and the mass of active material in one electrode, respectively. Specific capacitance derived from the CV tests[26] could be calculated using equation 2:

$$C = \frac{\int_{V_a}^{V_c} IdV}{m\upsilon(V_c - V_a)}, \tag{2}$$

where C(F·g^{-1}), I (A), m (g), υ (V·s^{-1}),V_c, and V_a are the specific capacitance,the instant current on CV curves, the mass of active electrode material in one electrode, the potential scan rate, and the high and the low potential limits of CV tests, respectively.

3 Results and discussion

3.1 The physical and chemical properties of the carbon monoliths

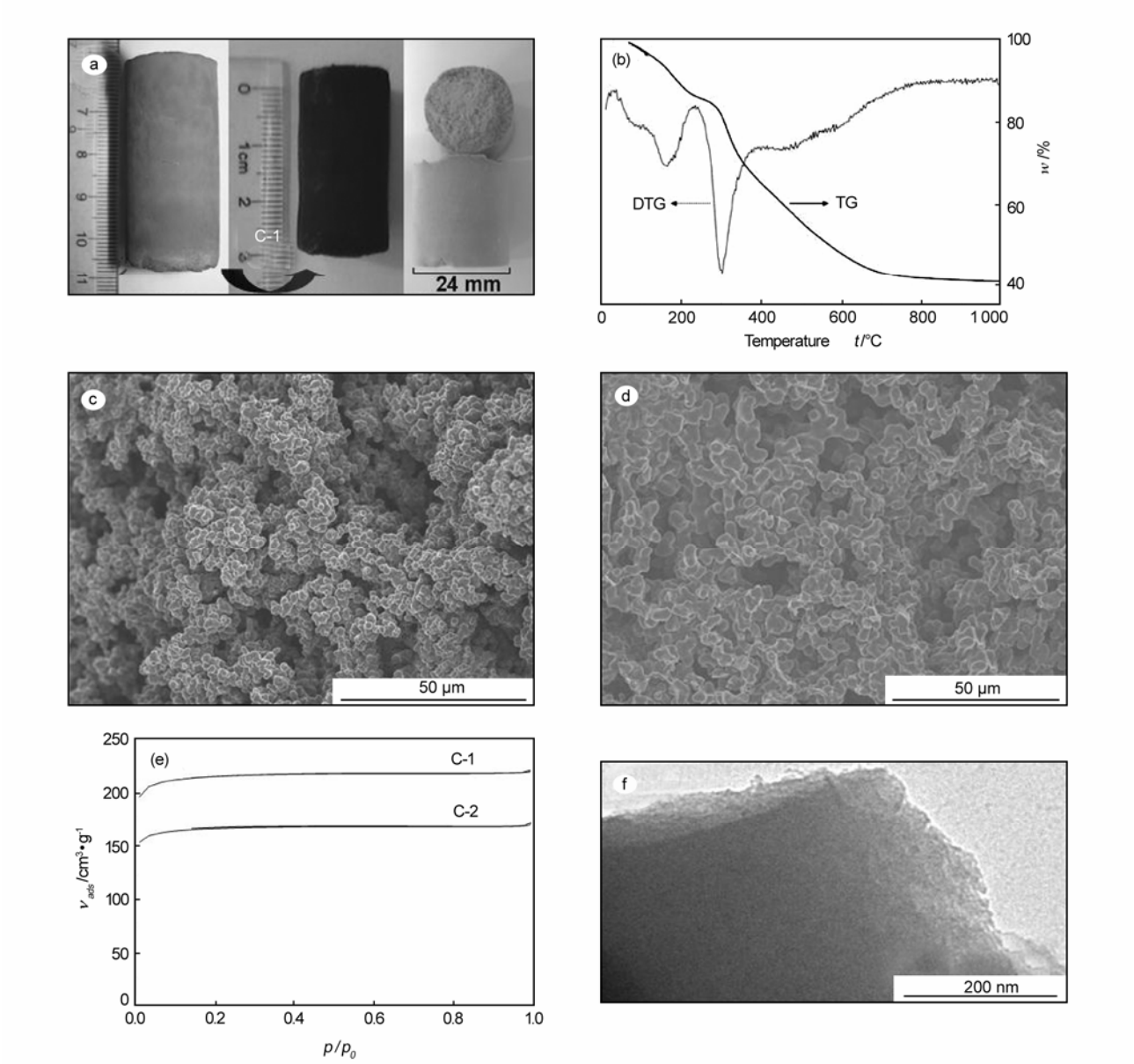

Fig.1 (a) Photographs of as-made polymer monolith (C-1 and C-2) and the carbonized product of C-1. (b) TG and DTG curves of the polymer sample of C-1. (c) SEM image of C-1. (d) SEM image of C-2. (e) N_2 sorption isotherms of C-1 and C-2. (f) TEM image of C-1

The macroscopic photograph of the polymer monoliths and the carbon monolith of C-1 are shown in Fig.1a. As can be seen, both the polymer monoliths are crack-free. The length and diameter of C-1 are 42 and 25 mm, respectively. After the carbonization process, a crack-free carbon monolith was obtained with a 28 mm length and a 17 mm diameter for C-1. The linear shrinkage along the longitudinal and the radial direction are about 33% and 32%, respectively. This indicates that the polymer structure is uniformly converted to carbon. TG-DTG curves as shown in Fig.1b reveal the thermal decomposition behavior of the C-1 polymer. The TG curve indicates a high yield of 40.2% for C-1, which is desirable in the synthesis of carbon materials. From the SEM images (Fig.1c&d), one can see that the skeletons of the carbon monoliths (both C-1 and C-2) consist of homogeneously interconnected spherical units, which create abundant macropores in the carbon framework, allowing an easy diffusion of the electrolyte ions. The N_2 sorption isotherms (Fig.1e) of C-1 and C-2 are both of type I, indicating a microporous characteristic that is beneficial to charge accumulation. The TEM image (Fig.1f) of C-1 further reveals that the carbon matrix is homogeneous with no detectable mesopores. As seen in Table 1, the specific surface areas are 722 and 556 $m^2 \cdot g^{-1}$, for C-1 and C-2, respectively. The micropore fractions of C-1 and C-2 are 88% and 89%, respectively. The abundant accessible micropores are expected to give a large storage capacity of electrolyte ions, thus leading to a high specific capacitance.

3.2 Electrochemical performance

Owing to the unique features such as highly interconnected porosity and abundant micropores, our nitrogen-containing carbon monoliths are investigated as electrodes for supercapacitors. To quantify the rate performance of

Table 1 The physical, chemical and electrochemical properties of the carbon monoliths

Sample	S_{BET}/m^2·g^{-1}	v_{total}/cm^3·g^{-1}	φ_{micro} /%	Nitrogen content	w/%	C^a/F·g^{-1}
C-1	722	0.34	88	0.82		199
C-2	556	0.27	89	0.31		83

[a] The specific capacitance of single electrode calculated from CV curves using equation 2.

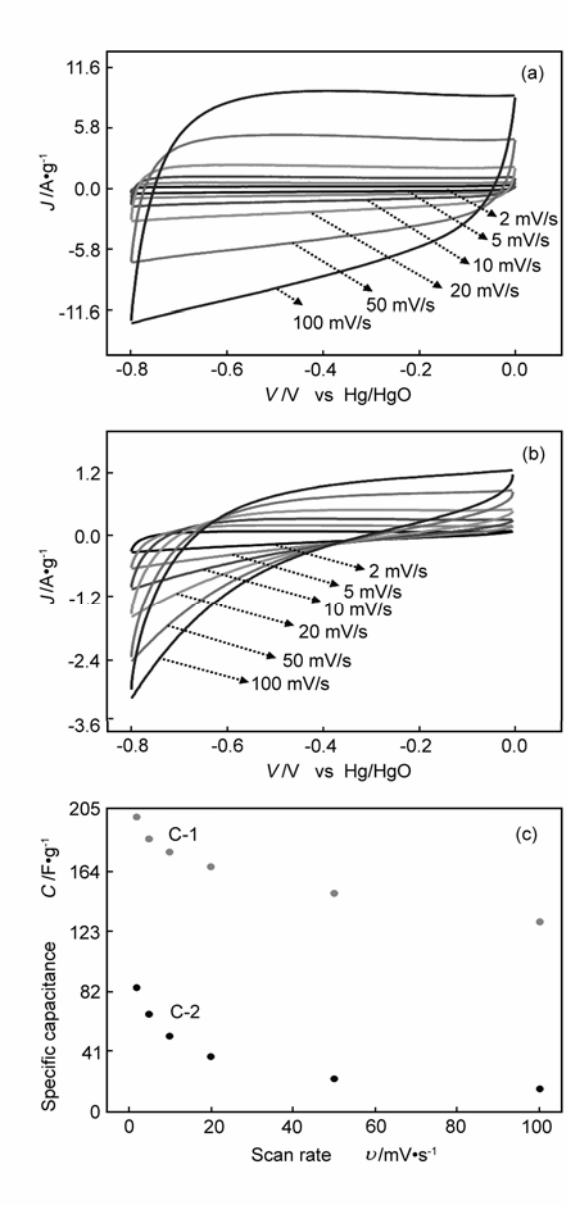

Fig.2 (a) The CV curves of C-1 electrode. (b) The CV curves of C-2 electrode. (c) Specific gravimetric capacitance of C-1 and C-2 electrodes at different scan rates, calculated from CV curves

C-1 and C-2 electrodes, CV are conducted at scan rates of 2, 5, 10, 20, 50, and 100 mV·s^{-1} with potential windows ranging from -0.8 to 0 V versus Hg/HgO in a 6 mol·L^{-1} KOH aqueous solution. Fig.2a shows the CV curves of the C-1 electrode at different scan rates. No pronounced reversible redox peak can be observed from CV curves of the C-1 electrode. In this case, charge storage is mainly electrostatic and the current is independent of the voltage. The shape of these curves is quasi-rectangular especially at a high scan rate of 100 mV·s^{-1}, indicating an ideal EDLC behavior and a fast charging/discharging characteristic, which are attributed to its 3D bicontinuous hierarchical porosity and abundant micropores.

Meanwhile, the C-2 electrode was measured with CV tests. As shown in Fig.2b, the shape of its CV curves shows a seriously deviated form of the rectangular one, which is quite different from the C-1 electrode. In general, at the same scan rate, a larger area of the CV curve indicates a higher specific capacitance of the capacitors. The calculated specific capacitances of C-1 and C-2 electrodes from the CV curves at different scan rates are shown in Fig.2c. At the scan rate of 2 mV·s^{-1}, the C-1 electrode has a specific capacitance of 199 F·g^{-1} (based on the mass of C-1 active material). At a high scan rate of 100 mV·s^{-1}, the specific capacitance of the C-1 electrode can be retained at 128 F·g^{-1}. However, at a scan rate of 2 mV·s^{-1} and 100 mV·s^{-1}, the specific capacitance of C-2 electrode achieves only 83 F·g^{-1} and 14 F·g^{-1}, respectively, which are much smaller than that of the C-1 electrode.

As known, the specific capacitance of electrode materials is related to the BET surface area and the pore structure. The specific surface area of the C-1 electrode as shown in Table 1 is as high as 722 m^2·g^{-1}, which is higher than that of the C-2 electrode (556 m^2·g^{-1}). Besides, the doping nitrogen can improve the wettablility and modify the electronic properties of the nitrogen-doped carbon materials. Frackowiak and coworkers[27] found that the doping heteroatom in porous carbons (e.g. containing N, O) improves their electrochemical performance. The elemental analysis reveals that the nitrogen content of the C-1 electrode is 0.82%, which is much higher than that of the C-2 electrode (0.31%). This high nitrogen content helps to improve the wettability of the carbon material, which facilitates the infiltration of the electrolyte ions into the interior pores, thereby enhancing the effective utilization rate of surface area, thus increasing the EDLC capacitance.

Fig.3 shows the charge-discharge curves of the C-1 and C-2 electrodes at a current density of 1.5 A·g^{-1}. The C-1 electrode shows a nearly linear charge-discharge curve, which indicates an ideal EDLC behavior with a specific capacitance of 116 F·g^{-1} calculated from GC curves with equation 1. Whereas, at the same condition, the C-2 electrode gives a capacitance of 32 F·g^{-1}, which is much lower than that of the C-1 electrode. The shape of the GC curves of the C-2 electrode deviated badly from an isosceles triangle. Moreover, the C-1 electrode exhibits a lower equivalent series resistance (ESR) than the C-2 electrode as shown from GC curves of Fig.3. A small ESR is essential to achieve a high rate capability or power density.

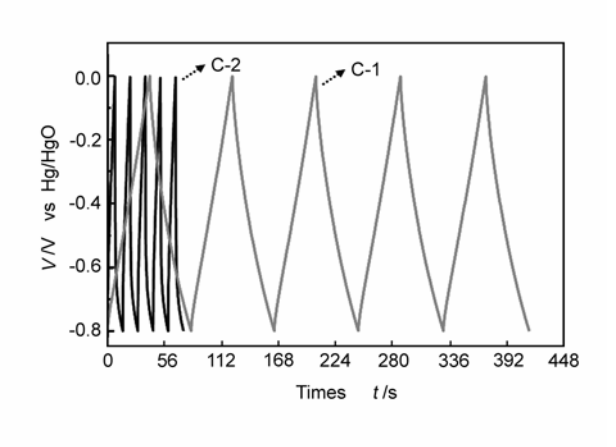

Fig.3 GC curves of the C-1 and C-2 carbon electrodes at a current density of 1.5 A·g^{-1}

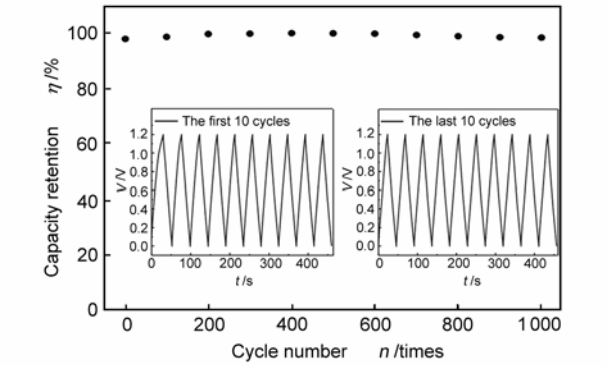

Fig.4 Charge/discharge cycling test at a current density of 1.5 A·g^{-1}, showing 1.6% loss after 1 000 cycles; inset shows the galvanostatic charge/discharge cyclic curves of the first and last 10 cycles

An important criterion for EDLCs is its cycling life. The cycling life tests over 1 000 cycles for the C-1 electrode at a current density of 1.5 A·g^{-1} were carried out using constant current GC techniques in the potential windows ranging from 0 to 1.2 V. Fig.4 shows the specific capacitance retention of the C-1 electrode as a function of charge/discharge cycling numbers. The C-1 electrode showed only a 1.6% loss in the specific capacitance after 1 000 charge-discharge cycles and the GC curves of the last 10 cycles had almost the same shape as that of the GC curves with the first 10 cycles (Fig.4 insets) and they had a very symmetric nature, illustrating again that the C-1 electrode has a good electrochemical capacitive characteristic and an excellent long-term cycling stability.

The distinct electrochemical properties of this two types of carbons with similar physical properties may also be caused by the bonding forms of heteroatoms (chemical environment) in the final products. Our ongoing works focus on distinguishing the nitrogen-containing functionalities by techniques such as solid NMR and XPS, and further revealing the possible correlations between the combined effects (both structure and nitrogen bonding forms) and electrochemical performance.

4 Conclusion

The electrochemical properties of two types of nitrogen-doped carbon monliths with hierarchical porosity over multi-length scale pores (ranging from nanometer to tens of micrometer) were investigated by means of cyclic voltammetry and galvanostatic charge/discharge techniques. Compared with the inorganic base catalyzed carbons with similar structures, L-lysine-incorporated carbons show high capacitance because of the higher nitrogen content, higher surface area, abundant micropores, and fully interconnected 3-D macropores, which shorten the diffusion route of electrolyte ions. The capacitance of C-1 can reach 199 F·g^{-1} in aqueous electrolytes. Combining the unique features and the good electrochemical performance, lysine-incorporated carbons are a promising candidate as the electrode material for EDLCs. The distinct electrochemical behavior of the two types of nitrogen-doped carbons also reveals that different precursors lead to entirely different existing forms of heteroatoms (chemical environment) in the final products, and thus affects the electrochemical performance.

Acknowledgments

The project was supported by the Program for New Century Excellent Talents in University of China (NCET-08-0075) and the Scientific Research Foundation of Ministry of Education of China for the Returned Overseas Chinese Scholars.

References

[1] Simon P, Gogotsi Y. Materials for electrochemical capacitors[J]. Nature Mater, 2008, 7: 845-854.

[2] Conway B E. Electrochemical Supercapacitors: Scientific Fundamentals and Technological Applications[M]. New York: Kluwer Academic/Plenum Publishers, 1999.

[3] Xing W, Qiao S Z, Ding R G, et al. Superior electric double layer capacitors using ordered mesoporous carbons[J]. Carbon, 2006, 44: 216-224.

[4] Kim N D, Kim W, Joo J B, et al. Electrochemical capacitor performance of N-doped mesoporous carbons prepared by ammoxidation[J]. J Power Sources, 2008, 180: 671-675.

[5] Ruiza V, Blanco C, Santamaría R, et al. An activated carbon monolith as an electrode material for supercapacitors[J]. Carbon, 2009, 47: 195-200.

[6] Gamby J, Taberna P L, Simon P, et al. Studies and characterisations of various activated carbons used for carbon/carbon supercapacitors[J]. J Power Sources, 2001, 101: 109-116.

[7] Zhu Y, Hu H, Li W C, et al. Cresol-formaldehyde based carbon aerogel as electrode material for electrochemical capacitor[J]. J Power Sources, 2006, 162: 738-742.

[8] Li W, Reichenauer G, Fricke J. Carbon aerogels derived from cresol-resorcinol-formaldehyde for supercapacitors [J]. Carbon 2002; 40: 2955-2959.

[9] Xia K, Gao Q, Jiang J, et al. Hierarchical porous carbons with controlled micropores and mesopores for supercapacitor electrode materials[J]. Carbon, 2008, 46: 1718-1726.

[10] Li J, Wang X, Wang Y, et al. Structure and electrochemical properties of carbon aerogels synthesized at ambient temperatures as supercapacitors[J]. J Non-Cryst Solids, 2008, 354: 19-24.

[11] Xing W, Huang C C, Zhuo S P, et al. Hierarchical porous carbons with high performance for supercapacitor electrodes[J]. Carbon, 2009, 47: 1715-1722.

[12] Dou Y Q, Zhai Y, Liu H, et al. Syntheses of polyaniline/ordered mesoporous carbon composites with interpenetrating framework and their electrochemical capacitive performance in alkaline solution[J]. J Power Sources, 2011, 196: 1608-1614.

[13] Wang D, Li F, Liu M, et al. Improved capacitance of SBA-15 templated mesoporous carbons after modification with nitric acid oxidation [J]. New Carbon Materials, 2007, 22(4): 307-314.

[14] Chen Z, Qin Y, Weng D, et al. Design and synthesis of hierarchical nanowire composites for electrochemical energy storage[J]. Adv Funct Mater, 2009, 19: 3420-3426.

[15] Huang C W, Wu Y T, Hu C C, et al. Textural and electrochemical characterization of porous carbon nanofibers as electrodes for supercapacitors[J]. J Power Sources, 2007, 172: 460-467.

[16] Bao L, Zang J, Li X. Flexible Zn_2SnO_4/MnO_2 core/shell nanocable-carbon microfiber hybrid composites for high-performance supercapacitor electrodes[J]. Nano Lett, 2011, 11: 1215-1220.

[17] Chmiola J, Yushin G, Gogotsi Y, et al. Anomalous increase in carbon capacitance at pore sizes less than 1 nanometer[J]. Science, 2006, 313: 1760-1763.

[18] Frackowiak E, Beguin F. Carbon materials for the electrochemical storage of energy in capacitors[J]. Carbon, 2001, 39: 937-950.

[19] Lufrano F, Staiti P. Mesoporous carbon materials as electrodes for electrochemical supercapacitors[J]. Int J Electrochem Sci, 2010, 5: 903-916.

[20] Hulicova D, Kodama M, Hatori H. Electrochemical performance of nitrogen-enriched carbons in aqueous and non-aqueous supercapacitors[J]. Chem Mater, 2006, 18: 2318-2326.

[21] Frackowiak E, Lota G, Machnikowski J, et al. Optimisation of supercapacitors using carbons with controlled nanotexture and nitrogen content[J]. Electrochim Acta, 2006, 51: 2209-2214.

[22] Hulicova-Jurcakova D, Seredych M, Lu G Q, et al. Combined effect of nitrogen- and oxygen-containing functional groups of microporous activated carbon on its electrochemical performance in supercapacitors[J]. Adv Funct Mater, 2009, 19: 438-447.

[23] Yang X, Wu D, Chen X, et al. Nitrogen-enriched nanocarbons with a 3-D continuous mesopore structure from polyacrylonitrile for supercapacitor application[J]. J Phys Chem C, 2010, 114: 8581-8586.

[24] Stein A, Wang Z, Fierke M A. Functionalization of porous carbon materials with designed pore architecture[J]. Adv Mater, 2009, 21: 265-293.

[25] Hao G P, Li W C, Qian D, et al. Rapid synthesis of nitrogen-doped porous carbon monolith for CO_2 capture[J]. Adv Mater, 2010, 22: 853-857.

[26] Fan Z J, Yan J, Zhi L J, et al. A three-dimensional carbon nanotube/graphene sandwich and its application as electrode in supercapacitors[J]. Adv Mater, 2010; 22: 3723-3728.

[27] Frackowiak E, Lota G, Machnikowski J, et al. Optimisation of supercapacitors using carbons with controlled nanotexture and nitrogen content[J]. Electrochim Acta, 2005, 51: 2209-2214.